LINC01980 induced by TGF-beta promotes hepatocellular carcinoma metastasis via miR-376b-5p/E2F5 axis

Jiaqi Sheng
Tongji Hospital of Tongji Medical College of Huazhong University of Science and Technology
Enjun Lv
Tongji Hospital of Tongji Medical College of Huazhong University of Science and Technology
Huifang Liang
Tongji Hospital of Tongji Medical College of Huazhong University of Science and Technology
Haisu Tao
Tongji Hospital of Tongji Medical College of Huazhong University of Science and Technology
Chengpeng Yu
Tongji Hospital of Tongji Medical College of Huazhong University of Science and Technology
Dean Rao
Tongji Hospital of Tongji Medical College of Huazhong University of Science and Technology
Mengyu Sun
Tongji Hospital of Tongji Medical College of Huazhong University of Science and Technology
Limin Xia
Tongji Hospital of Tongji Medical College of Huazhong University of Science and Technology
Wenjie Huang (huangwenjie@tjh.tjmu.edu.cn)
Tongji Hospital of Tongji Medical College of Huazhong University of Science and Technology
https://orcid.org/0000-0003-3182-8516

Research Article

Keywords: Long noncoding RNA, Metastasis, Hepatocellular carcinoma, TGF-β

Posted Date: May 18th, 2022

DOI: https://doi.org/10.21203/rs.3.rs-1622503/v1

Abstract

Hepatocellular carcinoma is one of the most aggressive human malignancies worldwide. However, the molecular mechanism of HCC metastasis is largely unknown. LncRNA has key roles in gene regulation, and dysregulation of lncRNA is critical to cancer metastasis. This study aims to explore the function and mechanism of LINC01980 in HCC metastasis and provides a new mechanism for transcription regulation of lncRNA. We first found that LINC01980 was upregulated and associated with poor prognosis in HCC. Besides, LINC01980 promoted HCC cells migration and invasion. Mechanistically, we proved that LINC01980 competitively bound miR-376b-5p to upregulate its target E2F5, thus inducing EMT in HCC cells. And, LINC01980-mediated HCC metastasis was dependent on E2F5 in vitro and vivo. In addition, our study showed that TGF-β activated LINC01980 transcription through the canonical TGF-β/SMAD signaling pathway in HCC. Overall, this study provided a new perspective to understand HCC metastasis and offered a new potential target for treating hepatocellular carcinoma.

Introduction

Hepatocellular carcinoma (HCC) is one of the most common human malignancies worldwide and the fourth leading cause of cancer-related death [1, 2]. Hepatitis B virus and hepatitis C virus infection are the main risk factors for HCC development, but non-alcoholic steatohepatitis is becoming a more significant risk factor in the West [3]. At present, surgical resection is the most effective treatment, with recognized curative potential [4]. Even so, the overall survival and prognosis for HCC patients remain unsatisfactory due to the high postoperative recurrence rate [5, 6]. Further investigations of HCC could enhance our understanding of the mechanisms associated with tumorigenicity and progression, and help us identify more effective therapeutic strategies.

Epithelial-mesenchymal transition (EMT) is a developmental program thought to involve a loss of epithelial features and acquire malignant traits by dedifferentiating into a mesenchymal phenotype, such as a loss of epithelial marker E-cadherin and a gain of mesenchymal marker vimentin [7, 8]. The mesenchymal state allows the cells to migrate to distant organs and maintain stemness, and subsequently differentiate into multiple cell types, thus EMT is of critical importance to endow cells with a more invasive potential during tumor cell metastatic dissemination [7]. Transforming growth factor beta (TGF-β), a multifunctional cytokine, involves in an intricate signaling network to modulate tumorigenesis and progression [9] and classically induces the activation of the SMAD complex to promote the transcription of hundreds of protein-coding and non-coding genes and then give rise to cancer metastasis [10–12]. In addition, TGF-β/SMAD signaling pathway often promotes tumor migration and invasion by inducing EMT [13]. Recently, several long non-coding RNAs (lncRNAs) are demonstrated to be involved in the canonical TGF-β signaling pathway and cancer metastasis [14–16]. However, whether lncRNAs are involved in the TGF-β/SMAD signaling and SMADs transcriptional regulation during HCC tumorigenesis and metastasis is still poorly understood.

LncRNAs are transcripts more than 200 nucleotides in length [17, 18]. LncRNAs constitute a large portion of the mammalian transcriptome and have key roles in gene regulation. Depending on their localization

and their interactions with DNA, RNA, and proteins, lncRNAs can modulate chromatin function, alter the stability and translation of cytoplasmic mRNAs and interfere with signal pathways [19, 20]. Many lncRNAs function as competing endogenous RNAs (ceRNAs) to regulate gene expression, thereby reducing microRNAs (miRNAs) availability to target mRNAs [21, 22]. These functions ultimately affect the expression of target genes and cause a variety of pathophysiological disorders, such as neuronal disorders, immune responses, cancers and so on [19]. Further, dysregulation of non-coding RNAs, including lncRNAs and miRNAs, is critical to cancer metastasis [23, 24]. For example, lncRNA PTAR promotes EMT and metastasis by competitively binding miR-101-3p to regulate ZEB1 expression in serous ovarian cancer [25]. To explore novel metastasis-associated lncRNAs in HCC, bioinformatics methods were used and LINC01980 was identified as a significant tumor promoter. Although LINC01980 may be implicated in the tumorigenesis and progression of esophageal squamous cell carcinoma (ESCC) [26], the mechanisms underlying its function in HCC are still unknown. Here, we found that LINC01980 acted as a ceRNA of miR-376b-5p to increase the expression of E2F5 indirectly, thereby promoting HCC metastasis. In addition, this study focused on the role of LINC01980 in canonical TGF-β/SMAD pathway.

Materials And Methods

Patients and tissue specimens

Liver tumor and adjacent non-tumor tissues were collected from HCC patients who underwent hepatectomy at the Hepatic Surgery Center, Tongji Hospital of Huazhong University of Science and Technology. The procedures were approved by the Ethics Committee of Tongji Hospital and conducted in terms of the Declaration of Helsinki Principles. The prior written and informed consent were obtained from all the patients.

Cell lines and cell culture

HCC cell lines, MHCC-97H (97H) and MHCC-LM3 (LM3), were obtained from Liver Cancer Institute of Zhongshan Hospital of Fudan University (Shanghai, China). Hep3B, Huh7, PLC/PRF-5, HLF and HepG2 were purchased from China Center for Type Culture Collection (CCTCC, Wuhan, China). All cell lines were cultured in Dulbecco Modified Eagle Medium (DMEM) (Hyclone, UT, USA) containing 10% fetal bovine serum (FBS) (Gibico) at 37 °C in a 5% CO2 cell incubator.

Cell transfection and lentivirus construction

The pcDNA3.1 vector (Invitrogen, USA) containing the full-length cDNA sequences of LINC01980 or E2F5 and pLKO.1 vector (Addgene, Cambridge) containing corresponding short hairpin RNA (shRNA) were provided by Tsingke Biological Technology (Beijing, China). The empty pcDNA3.1 vector and scramble shRNA were utilized as negative controls. All the siRNAs, miR-376b-5p mimics and miR-376b-5p inhibitors were designed by RiboBio (Guangzhou, China). Lipofectamine 3000 (Thermo Fisher Scientific, Waltham, MA, United States) was used as the transfection reagent according to the manufacturer's protocol. To construct gene over-expression cells lines, full-length sequence of LINC01980 was cloned into the

NheI/XhoI sites of pLenti-CMV-blast plasmid. All the overexpressing or silencing lentiviruses were produced in 293T cells by co-transfection of pMD2.G (Addgene #12259), psPAX2 (Addgene #12260) and pLenti-CMV-blast or pLKO.1-shRNA plasmids. 48 hours after transfection, virus supernatant was collected and filtered through a 0.45 μm filter. Then, the supernatant was used to transfect HCC cells with 8 μg/ml polybrene. 48 hours after transduction, infected cells were selected using puromycin (5 μg/mL) or blasticidin (10μg/ml) for 1 week.

Fluorescence in situ hybridization (FISH)

FISH assay was performed to detect the location of LINC01980 in HCC cells, using Fluorescent In Situ Hybridization Kit (RiboBio, Guangzhou, China) according to the manufacturer's instructions. LINC01980-specific probes were designed by RiboBio (Guangzhou, China). Briefly, LM3 cells were fixed with 4% paraformaldehyde for 10 minutes at room temperature and permeabilized with 0.5% TritonX-100 for 5 minutes at 4°C. Prehybridization was performed with lncRNA FISH probe mix at 37°C for 30 minutes. Subsequently, hybridization was performed with LINC01980-specific probes mix, incubating the mixture overnight at 37°C. After washing with 4X, 2X, and 1X SSC by steps, cell nuclei were stained with DAPI and acquired images by confocal microscope (Olympus).

Quantitative real-time PCR (qRT-PCR)

Total RNAs of tissues and cells were extracted by TRIzol reagent (Takara, Japan) according to the manufacturer's instructions. Reverse-transcribed complementary DNA of lncRNA and mRNA was synthesized using the HiScript® II Q RT SuperMix for qPCR (Vazyme Biotech Co., Ltd). And for miRNA, reverse transcription was performed using the Mir-X miRNA First-Strand Synthesis Kit (Takara, Japan). Quantitative real-time PCR was performed using ChamQ Universal SYBR qPCR Master Mix (Vazyme Biotech Co., Ltd) following the protocol with CFX Connect™ real time system (Bio-Rad, USA). Differential analysis between samples was determined by the $2-\Delta\Delta Ct$ method. All reactions were performed as triplicates, independently of each other. Primers were designed using NCBI Primer-BLAST and gene-specific primers used in this study were listed in Supplementary Table 1.

Transwell migration and invasion assay

24-well transwell plate with 8 μm pore size polycarbonate membrane (Corning, NY, USA) was used to evaluate cell migration and invasion ability. HCC cells (3×10^4 Hep3B, HLF, 97H cells and 2×10^4 LM3 cells for migration assays; 6×10^4 Hep3B, HLF, 97H cells and 4×10^4 LM3 cells for invasion assays) were planted in the upper chamber precoated with Matrigel (BD bioscience, NJ, USA; without Matrigel for cell migration assay), and 600μl DMEM media containing 10% FBS were added to the lower chamber. After a 24 h incubation at 37 °C, non-migrated or non-invaded cells inside the upper chamber were obliterated with cotton swabs, while cells on the lower membrane surface were fixed with 4% paraformaldehyde and then stained with 0.5% crystal violet solution. Five fields were counted randomly in each well. Three random areas in each chamber were captured with an optical microscope (Leica) under 100x magnification.

Western blot

Total protein from HCC cells was extracted by RIPA buffer supplemented with protease and phosphatase inhibitor cocktail (MedChemExpress, USA) on ice for 30 min. The protein concentration was quantitated using a BCA protein quantification kit (Thermo Fisher Scientific). Subsequently, equal amounts (20 μg/lane) of protein were separated by 10% SDS-PAGE (Boster Biological Technology, Wuhan, China) and transferred to polyvinylidene fluoride (PVDF) membranes (Millipore, USA). Then, the membranes were blocked with 5% skim milk at room temperature for 1 h and incubated with primary antibodies anti-E2F5 (1:500, sc-9976, Santa Cruz Biotechnology, USA) and β-actin (1:1000, #4967BC, Cell Signaling Technology, USA) at 4 °C overnight. Subsequently, the membranes were incubated with secondary antibody (1:5000, Promoter, China) at room temperature for 1 h. Finally, immunoreactive bands were visualized with ECL chemiluminescent kit (Bio-Rad, USA). Blot densitometric analysis was performed by Image Lab™ 4.0 software (Bio-Rad Laboratories).

Dual luciferase assay

The sequence of LINC01980 and 3'UTR of the E2F5 targeted by miR-376b-5p and their corresponding mutation were respectively designed, synthesized and cloned into luciferase reporter vector psiCHECK-2 (Promega, Madison, WI, USA). About 1×10^5 HCC cells/well were seeded into 24-well plates. After 12h, cells were co-transfected with 100 ng of the psiCHECK-2 vector and 50 nM of the miR-376b-5p mimic or NC-mimic using Lipofectamine 3000 (Invitrogen, USA). After 48 h of co-transfection, cells were lysed by Passive Lysis Buffer (Promega, USA), and the relative luciferase activity was measured by Dual Luciferase Assay Kit (Promega, USA) according to the manufacturer's instructions.

RNA immunoprecipitation (RIP)

RNA immunoprecipitation assay was performed by the Magna RIP™ RNA-Binding Protein Immunoprecipitation Kit (Millipore, Germany), according to the manufacturer's instruction. Rabbit anti-Ago2 was purchased from Abcam (ab186733) and IgG was used as a negative control. The immunoprecipitated RNA was purified and further subjected to qRT-PCR analysis. The $2^{-\Delta CT}$ was calculated and normalized by the $2^{-\Delta CT}$ of 10% input.

Biotinylated RNA Pull-down assay

The entire experimental process should be performed in the RNase-free conditions. Biotin labeled LINC01980 and antisense-LINC01980 control transcripts were obtained respectively from linearized pcDNA3.1-LINC01980 or pcDNA3.1-LINC01980 antisense plasmid by vitro transcription, using the Ribo™ RNAmax-T7 Biotin Labeling Transcribe Kit (RiboBio, Guangzhou, China). Subsequently, 100 pmol of purified biotin-labeled transcripts were incubated with cell lysates from 2×10^7 Hep3B cells for 1h at room temperature, which was treated with Ribonuclease Inhibitor. Then, Streptavidin Magnetic Beads (Thermo Fisher Scientific, Waltham, MA, United States) were added to isolate the biotin-labeled RNAs by incubating with rotation at 4°C for 2h. The enrichment of RNA was detected by qRT-PCR analysis.

Chromatin immunoprecipitation assay (ChIP)

ChIP assay was performed using the Chromatin Immunoprecipitation Kit (CST) according to the manufacturer's protocol. Briefly, Hep3B or HLF cells (3.0 x 10^7 cells) were crosslinked with 1% formaldehyde at room temperature for 10 min, and the crosslinking was terminated by adding 0.125 M glycine. After washing cells twice with PBS, cells were lysed with lysis buffers and sonicated to yield 150-250 bp DNA fragments. Immunoprecipitations were carried out using anti-SMAD3 and IgG as the control. The immunoprecipitated DNA fragments and the input were then purified and detected by real-time PCR assays using primers targeting the LINC01980 promoter region that encompassed the SMAD3 binding site. ChIP primers used for L4 region of LINC01980 promoter were as follows: L4-F: 5'-CTTGAGCCCAAATGAGCACA -3' and L4-R: 5'- TATCAGCCCGCTCCTTCTTC -3'.

Lung metastasis models

The animal experiment was performed in accordance with the guidelines of the care and use of laboratory animals, and approved by the Ethic Committee of Tongji Hospital of Huazhong University of Science and Technology. Before the experiments, luciferase-labeled HCC cells with LINC01980 stably overexpressing or silencing, and the negative control cell lines were constructed. In addition, E2F5 stably silencing cell lines or the control cell lines, in the base of LINC01980 stably overexpressing cell lines or vector cell lines, were also established. Next, HCC cells (1×10^6) were injected into the tail veins of 6-week-old male BALB/C nude mice and each group had six mice. All the mice groups were sacrificed 6 or 8 weeks after injection, and the lungs of each mouse were separated and observed by the IVIS, Lumina XRMS, Series III (PerkinElmer, USA) with the help of D-Luciferin (Caliper Life Sciences, Waltham, MA USA). Then, the lungs were fixed for hematoxylin and eosin (H&E) staining and the H&E pictures obtained by OCUS.

Results

LINC01980 is highly expressed and related to poor prognosis in HCC

To reveal novel lncRNAs involved in the development of HCC, a LIHC cohort derived from TCGA was analyzed, which contained 374 tumor samples and 50 normal samples, and 3129 differentially expressed lncRNAs were discovered (Supplementary Table 2). In this study, we mainly focused on the up-regulated top 20 lncRNAs (Fig. 1A), of which HOTTIP [27], DSCR8 [28], LINC01287 [29] were proven to promote HCC progression. And we selected LINC01980 for further investigation, which recently had been reported in ESCC [26] but the mechanisms underlying its function in HCC are still unknown. Through analyzing the TCGA database, we found that LINC01980 was significantly upregulated in HCC tissues compared with that in normal liver tissues (Fig. 1B). In addition, by analyzing the relationship between the expression of LINC01980 and the pathological tumor grade or stage, it was found that the expression of LINC01980 was positively correlated with the tumor grade and stage of HCC patients (Fig. 1C and D). To study the effect of LINC01980 expression on the prognosis of HCC patients, survival analysis was carried out, and the results showed that the overall survival of HCC patients with high LINC01980 expression was significantly worse than that of patients with low expression (Fig. 1E). Subsequently, the qRT-PCR results getting from fifty pairs of HCC tissue samples confirmed the high expression of LINC01980 in HCC tissues compared with adjacent non-tumor tissues (Fig. 1F and G).

In addition, the potential clinical significance of LINC01980 in HCC was explored, by analyzing the relationship between the expression of LINC01980 in fifty pairs of HCC tissue samples and corresponding clinical characteristics of those patients. The results showed that HCC patients with LINC01980 high expression were more likely to lead to extrahepatic ($p = 0.015$) and lymphatic ($p = 0.037$) metastasis, compared with patients with LINC01980 low expression (Table 1). Furthermore, the expression of LINC01980 in HCC cell lines with different metastasis potential was assessed via qRT-PCR, and the result showed that LINC01980 was relatively high expression in LM3 and 97H cells with high metastatic potential, and relatively low expression in Hep3B and HLF cells with low metastatic potential (Fig. 1H).

Table 1

Correlation between LINC01980 or E2F5 and clinicopathological characteristics in 50 pairs of HCC patients.

Variable	All cases	LINC01980 expression		P value	E2F5 expression		P value
	(n=50)	Low expression	High expression		Low expression	High expression	
Age (years)							
≥50	22	12	10	0.568	7	15	**0.022***
<50	28	13	15		18	10	
Sex							
Male	41	21	20	0.713	21	20	0.713
Female	9	4	5		4	5	
Hepatitis							
Positive	35	19	16	0.355	19	16	0.355
Negative	15	6	9		6	9	
AFP (ng/mL)							
≤400	24	12	12	1.000	9	15	0.089
>400	26	13	13		16	10	
Liver cirrhosis							
Yes	41	23	18	0.066	20	21	0.713
No	9	2	7		5	4	
Tumor size (cm)							
≤5	22	11	11	1.000	9	13	0.254
>5	28	14	14		16	12	
Intrahepatic Metastasis							
Yes	19	8	11	0.382	7	12	0.145
No	31	17	14		18	13	
Extrahepatic Metastasis							
Yes	16	4	12	**0.015***	4	12	**0.015***
No	34	21	13		21	13	
Lymph Node							

Metastasis							
Yes	4	0	4	**0.037***	1	3	0.297
No	46	25	21		24	22	
Differentiation							
Well-moderated	12	5	7	0.508	4	8	0.185
Poor-undifferentiated	38	20	18		21	17	

AFP: alpha fetoprotein; P value was calculated by Chi-square test; *Statistically significant.

LINC01980 promotes HCC cell metastasis in vitro and vivo

To investigate the influence of LINC01980 on HCC cell metastatic abilities, Hep3B and HLF cell lines with LINC01980 stably overexpressing or LM3 and 97H cell lines with LINC01980 stably silencing were respectively constructed. The overexpressing or knocking down efficiency was confirmed by qRT-PCR analysis (Fig. 2A and B). Transwell assays showed that up-regulation of LINC01980 contributed to enhancing cell migration and invasion (Fig. 2C-E), whereas down-regulation of LINC01980 inhibited cell migration and invasion (Fig. 2F-H).

To further explore the ability of LINC01980 to promote HCC metastasis in vivo, HLF cell lines with LINC01980 stably overexpressing or 97H cell lines with LINC01980 stably silencing were injected into the tail veins of 6-week-old male BALB/C nude mice. The mice were sacrificed after being injected for 6 weeks. Representative bioluminescent imaging of the different groups is shown in Fig. 2I and L. Compared with the control group, more and stronger bioluminescence signals were found in the lung of LINC01980 overexpressed group (Fig. 2I). In contrast, LINC01980 silenced group showed fewer and weaker bioluminescence signals in the lung than those in the control group (Fig. 2L). The H&E staining analysis indicated that the LINC01980 overexpressed group formed more metastatic nodules in lungs than the control group (Fig. 2J and K), while the LINC01980 silenced group formed fewer metastatic nodules in lungs than the control group (Fig. 2M and N). In summary, LINC01980 promoted HCC cell metastasis in vitro and vivo.

LINC01980 acts as a ceRNA and competitively binds miR-376b-5p

To explore how LINC01980 performs its function in HCC, subcellular localization of LINC01980 in HCC cells was identified by nuclear-cytoplasmic RNA fractionation and FISH assays. The results showed that LINC01980 was localized mainly in the cytoplasm of HCC cells (Fig. 3A and B). Based on the results of subcellular localization, LINC01980 was hypothesized to function as a ceRNA that interacts with specific miRNAs and influences miRNA-mediated biological processes.

To explore the underlying mechanism, the miRNAs that bind with LINC01980 were predicted by LncBase Predicted v.2 (http://carolina.imis.athena-innovation.gr/diana_tools/web/index.php). As shown in Fig. 3C and D, sixteen potential target miRNAs were selected and qRT-PCR assays were conducted to screen the

target. The results showed that LINC01980 overexpressing only repressed miR-376b-5p expression among all the candidate genes in Hep3B and HLF cells. Conversely, LINC01980 silencing up-regulated miR-376b-5p expression in LM3 and 97H cells (Fig. 3E). Therefore, LINC01980 might be a ceRNA of miR-376b-5p. Their binding site was predicted by RNAhybrid (http://bibiserv.techfak.uni-bielefeld.de/rnahybrid/) and indicated in Fig. 3F, and a wild type (WT) and a mutated (MUT) LINC01980 luciferase reporter gene were respectively constructed (Fig. 3F). Then, the results of the dual-luciferase reporter assay showed that the luciferase activity was decreased when co-transfected with LINC01980-WT and miR-376b-5p mimic, while co-transfected with LINC01980-MUT and miR-376b-5p mimic displayed no difference (Fig. 3G and H).

Ago2 is a core component of the RNA-induced silencing complex (RISC) that participates in miRNA-mediating mRNA destabilization or translational repression. The Ago2-RIP assay was performed to determine the interaction between LINC01980 and miR-376b-5p. The results showed that endogenous LINC01980 was preferentially enriched in Ago2 compared with control IgG (Fig. 3I) and LINC01980 enrichment was more in miR-376b-5p overexpression groups than that in the miR-Ctrl group (Fig. 3J). These results indicated that LINC01980 and miR-376b-5p were in the same RISC. Moreover, RNA pulldown assays (Fig. 3K) showed that biotin-labeled LINC01980 can enrich more miR-376b-5p compare with antisense-LINC01980 control (Fig. 3L), which demonstrated that LINC01980 directly sponges miR-376b-5p. In addition, the expression of miR-376b-5p in 50 pairs of HCC and adjacent non-cancerous tissues was examined by qRT-PCR. The results showed that miR-376b-5p expression was significantly lower in HCC tissues than adjacent non-tumor tissues (Fig. 3M and N). Consistent with the results in the StarBase website, the expression of miR-376b-5p was lower in cancer tissues (Fig. 3O). To further explore the correlation between LINC01980 and miR-376b-5p, spearman's correlation analysis was performed, and miR-376b-5p expression was found to be negatively correlated with LINC01980 expression in tumor tissues (Fig. 3P), which is also consistent with the result analyzed by the StarBase website (Fig. 3Q).

E2F5 is a downstream target of miR-376b-5p

Considering that miRNAs exert their function by modulating the expression of target genes, three bioinformatics databases (miRDB, DIANA, and TargetScan) were used to predict the potential targets of miR-376b-5p. As shown in Fig. 4A, eleven targets were overlapping in the prediction results of these three databases. Among these genes, only APEX1[30, 31], E2F5 [32, 33], and NEF2L3 [34, 35] have been reported to contribute to the development of liver cancer and tumor metastasis. It is worth noting that only E2F5 expression was positively correlated with LINC01980 expression in HCC tissues through StarBase website analysis (Fig. 4B). According to the results obtained, E2F5 was chosen as our downstream target gene. Through the StarBase website analysis, it is found that E2F5 was overexpressed in cancer tissues (Fig. 4C). Subsequently, the expression of E2F5 in paired HCC tissue samples was detected. As expected, E2F5 was up-regulated in HCC tissue (Fig. 4D and E). And, the potential clinical significance of E2F5 in HCC was explored by analyzing the relationship between the expression of E2F5 in paired HCC tissue samples and corresponding clinical characteristics. The results showed that HCC patients with E2F5 high expression were more likely to predispose to extrahepatic metastasis ($p = 0.015$), compared with patients with E2F5 low expression (Table 1).

In addition, the expression of E2F5 was positively correlated with LINC01980 expression (Fig. 4F), while negatively correlated with miR-376b-5p expression (Fig. 4G). Moreover, the prognosis of HCC patients was explored by StarBase and Kaplan Meier-plotter websites, and the results certified that higher E2F5 expression predicted shorter overall survival (OS) in both patient cohorts (Fig. 4H and I). Subsequently, Ago2-RIP assays were conducted, and increasing enrichment of LINC01980 and decreasing enrichment of E2F5 transcript on Ago2 were observed in LINC01980 overexpressed HCC cells compared to the controls (Fig. 4J and K). The RIP results indicated that LINC01980 and E2F5 transcript could competitively bind miR-376b-5p in Ago2 (Fig. 4L). Taken together, E2F5 is a direct target of miR-376b-5p in HCC cells.

LINC01980 decoys miR-376b-5p to upregulate its target E2F5

MicroRNAs have often been reported to target the 3'-untranslated region (3' UTR) of mRNAs to perform functions [36]. Therefore, the potential binding site between miR-376b-5p and 3'UTR of E2F5 was predicted by the TargetScan database. The result showed that the position 207-214 of E2F5 3' UTR might bind with miR-376b-5p (Fig. 5A). Subsequently, a wild type (WT) and a mutated (MUT) E2F5 3'UTR dual luciferase reporter plasmids in psiCHEK2 were constructed respectively (Fig. 5A). Dual-luciferase reporter assay showed that miR-376b-5p mimic inhibited luciferase activity and the changes were abolished after mutating the binding site (Fig. 5B and C). Moreover, qRT-PCR and western blot demonstrated that overexpressing miR-376b-5p suppressed and knocking down miR-376b-5p promoted the E2F5 mRNA and protein expression (Fig. 5D and E). In conclusion, miR-376b-5p inhibited E2F5 expression through binding to its 3'UTR. In addition, upregulation and downregulation of LINC01980 also positively affected E2F5 expression at both the mRNA and protein levels (Fig. 5F and G). To further investigate the relationship among LINC01980, miR-376b-5p, and E2F5, rescue experiments were performed, and the result showed that the promotive effect of LINC01980 on E2F5 expression was attenuated by miR-376b-5p mimic (Fig. 5H). In contrast, miR-376b-5p inhibitor rescued the repressive effect of LINC01980 silencing on E2F5 expression (Fig. 5I). Moreover, the dual-luciferase reporter assays showed that the cotransfection of miR-376b-5p mimic and LINC01980 weakened the intensive role of LINC01980 to luciferase activity of E2F5 (Fig. 5J and K). Overall, these findings indicated the existence of a LINC01980/miR-376b-5p/E2F5 regulatory axis, and LINC01980 decoyed miR-376b-5p to upregulate its target E2F5.

E2F5 is indispensable for LINC01980-mediated HCC metastasis in vitro and vivo

To verify the ability of LINC01980 to promote tumor metastasis in an E2F5-dependent manner, rescue experiments were performed. First of all, Hep3B and HLF cells were transfected with E2F5 siRNAs (siE2F5-1 and siE2F5-2) against E2F5, while LM3 and 97H cells were transfected with E2F5-overexpressing plasmid. And the overexpressing or knocking down efficiency was confirmed by quantitative RT-PCR analysis and western blot assay (Supplementary Fig. 1A-D). Subsequently, Hep3B and HLF cells stably overexpressing LINC01980 or empty vector were transfected with E2F5 or control siRNA. On the contrary, LM3 and 97H cells stably silencing LINC01980 were transfected with E2F5 overexpression plasmid or empty vector. Transwell assays showed that inhibiting E2F5 expression partially attenuated the promotive effects of LINC01980 overexpression on HCC cell migration and invasion (Fig. 6A and B), while increasing E2F5 expression partially rescued the suppressive effects of LINC01980 knockdown on HCC cells

migration and invasion (Fig. 6C and D). Further, western blot assays showed that upregulating LINC01980 increased E2F5 and vimentin protein levels, and decreased E-cadherin protein expression in Hep3B and HLF cells. However, the change of protein level caused by LINC01980 overexpression was reversed by E2F5 siRNA (Fig. 6E). On the contrary, E2F5 overexpression reversed the suppressive effects of LINC01980 knockdown on the E2F5 and vimentin protein levels and abolished the promotive effects of LINC01980 knockdown on the E-cadherin protein levels (Fig. 6F).

As for the lung metastasis model, E2F5 stably silencing or the control cell lines were established in the base of LINC01980 stably overexpressing or control HLF cell lines. These four kinds of cell lines were injected into the tail veins of 6-week-old male BALB/C nude mice. Eight weeks after injection, the mice were sacrificed and representative bioluminescent imaging of the different groups is shown in Fig. 6G. Compared with the LINC01980 overexpressed group, fewer and weaker bioluminescence signals were shown in the lung of LINC01980 overexpressed group with E2F5 stably silencing (Fig. 6G). Furthermore, the H&E results showed that silencing E2F5 inhibited the formation of metastatic nodules caused by LINC01980 overexpression (Fig. 6H and I). Therefore, silencing E2F5 attenuated effective of LINC01980 to promote HCC metastasis in vivo. In summary, E2F5 was proved to be indispensable for LINC01980-mediated HCC metastasis in vitro and vivo.

LINC01980 is induced by the canonical TGF-β/SMAD signaling pathway

TGF-β functions as a potent metastasis stimulator by enhancing the EMT and cancer cell colonization in distant organs [9, 37]. To identify whether LINC01980 was responsive to TGF-β, the LINC01980 level in TGF-β-treated HCC cells was tested by qRT-PCR at different times. The results showed that LINC01980 was significantly induced at 12h after TGF-β treatment (Fig. 7A and B). To investigate whether the SMAD complex was involved in TGF-β-induced LINC01980 expression. Potential SMAD binding sites were predicted by using the online database hTFtarget (http://bioinfo.life.hust.edu.cn/hTFtarget/). It is found that four potential SMAD3/4 binding sites were on the LINC01980 promoter, which located at -1997/-1988 (L1), -1893/-1876 (L2), -1262/-1244 (L3), and -489/-472 (L4) nucleotides from the transcription start site (Fig. 7C). To confirm that LINC01980 was a transcriptional target of SMAD3/4, the promoter region of LINC01980 (-2036 to +64) was cloned into pGL4.17 luciferase reporter plasmid to generate the so-called L1-4 plasmid (Fig. 7C). Then, three different promoter truncations from the L1-4 plasmid were made, respectively containing the different portion of promoter (Fig. 7C): L2-4 (-1936/+64), L3-4 (-1,356/+64), and L4 (-586/+64). Luciferase reporter assay revealed that TGF-β significantly increased the activity of the 2.1-kb LINC01980 promoter and promoter truncations in Hep3B and HLF cells (Fig. 7D and E). And more notably, the luciferase activity of promoter truncation containing L4 binding site was still obviously enhanced by TGF-β (Fig. 7D and E). These results indicated that the L4 binding site might be indispensable for TGF-β-induced LINC01980 transcription. In order to prove this speculation, four potential SMAD3/4 binding sites were mutated, respectively (Fig. 7F). The luciferase reporter assay showed that only L4 mutation prevented luciferase activity from being affected by TGF-β (Fig. 7G and H). This result suggested that the L4 region was indispensable for LINC01980 promoter activities induced by TGF-β in Hep3B and HLF cells. To further prove the interaction between L4 region of the LINC01980 promoter and SMAD

complexs, chromatin immunoprecipitation assays (ChIP assays) were performed in Hep3B and HLF cells by using SMAD3 antibodies. The results showed that LINC01980 promoters were efficiently enriched by SMAD3 after TGF-β treatment (Fig. 7I-K). Taken together, these findings demonstrated that TGF-β directly activated LINC01980 transcription through the canonical TGF-β/SMAD signaling pathway in HCC.

Discussion

In recent years, accumulating evidence indicates that lncRNAs dysregulation is involved in the tumorigenesis and progression of various types of cancers [38], including hepatocellular carcinoma [39]. LINC01980 has been identified as a novel oncogene implicated in the tumorigenesis and progression of ESCC [26]. However, the role of LINC01980 in HCC has not been investigated. Here, we found that LINC01980 was upregulated and associated with notably worse overall survival in HCC patients. In addition, LINC01980 expression was positively correlated with both tumor grade and stage. And, HCC patients with LINC01980 high expression were more likely to lead to extrahepatic and lymphatic metastasis. Functionally, LINC01980 functioned as a tumor-promotor, contributing to HCC cell metastasis in vitro and in vivo. Therefore, LINC01980 plays a carcinogenic role in HCC progression, and may be used as a prognostic indicator for HCC patients.

The subcellular localization of lncRNAs can indicate the mechanism of their biological functions. LncRNAs located in the cell nucleus perform their function through binding with particular target proteins, while lncRNAs located in the cytoplasm generally regulate gene expression at the post-transcriptional level through the ceRNA mechanism [40]. In this study, LINC01980 was found to mainly locate in the cytoplasm, so it might exert its oncogenic role in HCC cells through functioning as a ceRNA. As expected, miR-376b-5p, a new potential target miRNA of LINC01980, was found by bioinformatics software. And through qRT-PCR, luciferase reporter assay, Ago2-RIP, and RNA pulldown assay, LINC01980 was further verified to bind miR-376b-5p directly. Correlation analysis showed that miR-376b-5p expression was negatively regulated by LINC01980 in HCC. In summary, LINC01980 can sponge miR-376b-5p in HCC.

Growing evidence supports the existence of an extensive interaction network involving ceRNAs, in which lncRNAs regulate mRNAs expression by competitively binding miRNAs [41–43]. For example, lnc-TALC functions as a ceRNA to regulate c-Met by competitively binding with miR-20b-3p to promote methyltransferase expression [42]. FAM225A promotes NPC cell proliferation, migration, and invasion by acting as a ceRNA that sponges miR-590-3p and miR-1275 to regulate ITGB3 expression [41]. In this study, several potential target mRNAs of miR-376b-5p were found by using bioinformatics analysis, of which only E2F5 expression was positively correlated with LINC01980 expression and upregulated in HCC tissues. Combining with the results of qRT-PCR and correlation analysis in our cohort, E2F5 was confirmed to be a new target of miR-376b-5p in HCC. Moreover, the prognostic analysis demonstrated that higher expression of E2F5 predicted shorter overall survival in HCC. The Ago2-RIP assay further certified that LINC01980 and E2F5 transcript could competitively bind miR-376b-5p in Ago2. Taken together, E2F5 is a direct target of miR-376b-5p in HCC cells.

E2F transcription factor 5 (E2F5), as a member of the E2F family, is widely involved in the development and progression of various tumors, including hepatocellular carcinoma [32, 44]. For example, E2F5 was confirmed to promote prostate cancer cell migration and invasion through regulating TFPI2, MMP-2, and MMP-9 [33]. What's more, MALAT1 could increase DDP resistance, and promote migration and invasion by sponging miR-1271-5p to upregulate E2F5 expression in DDP-resistant OC cells [45]. Therefore, there was speculation that LINC01980 was associated with HCC metastasis in an E2F5-dependent manner. Moreover, because of miRNAs binding to 3'UTR of target mRNAs and making it instability and degradation [36, 41, 42], dual-luciferase reporter assays were firstly carried out. The results verified that miR-376b-5p inhibited the activity of E2F5 by binding to its 3'UTR. Secondly, the expression of E2F5 was negatively regulated by miR-376b-5p while positively regulated by LINC01980 in HCC cells. Simultaneously, the effect of LINC01980 on E2F5 expression was attenuated by miR-376b-5p. Finally, a series of rescue experiments were conducted and illustrated that E2F5 mediated the prometastatic function of LINC01980 in vitro and vivo. Taken together, these findings indicated the existence of a LINC01980/miR-376b-5p/E2F5 regulatory axis and further demonstrated that LINC01980 could promote migration and invasion by sponging miR-376b-5p to increase E2F5 expression in HCC cells.

Interestingly enough, previous researches have shown that TGF-β induces several lncRNAs, including ELIT-1, HCP5, lncRNA-ATB, and lncRNA-Smad7, all of which are involved in cellular responses elicited by TGF-β and participated in EMT [12, 46–48]. However, there has been no report about lncRNA that is mediated transcription by the canonical TGF-β/SMAD pathway in HCC. Our study showed that LINC01980 was induced by TGF-β. Moreover, luciferase reporter assays and ChIP assays demonstrated that LINC01980 transcription was directly regulated by SMAD3. In conclusion, TGF-β activated LINC01980 transcription through the canonical TGF-β/SMAD signaling pathway in HCC.

In summary, our study showed that LINC01980 promoted HCC metastasis via competitively binding miR-376b-5p to upregulate its target E2F5, thus inducing EMT in HCC cells. Moreover, TGF-β activated LINC01980 transcription through the canonical TGF-β/SMAD signaling pathway in HCC (Fig. 7L). This work provided a new perspective to understand HCC metastasis and offered a new potential target for treating hepatocellular carcinoma.

Declarations

Funding

This work was supported by National Natural Science Foundation of China, No. 82173313 and No. 81871191.

Competing interests

The authors declare that they have no competing interests.

Author contributions

Jiaqi Sheng designed the experiments, analyzed the data, and wrote the manuscript. Jiaqi Sheng, Enjun lv, Chengpeng Yu, and Dean Rao performed the experiments. Haisu Tao and Mengyu Sun conducted bioinformatic analysis and statistical analysis. Huifang Liang provided technical and material support. Limin Xia and Wenjie Huang analyzed research data, revised the manuscript, and obtained funding. All of the authors discussed the results and approved the final manuscript.

Data Availability

All the data supporting the conclusions were included in the main paper.

Ethics approval and consent to participate

The human samples were obtained from Tongji hospital with the guidance of the Declaration of Helsinki and this study was approved by the Medical Ethics Committee of Tongji Hospital. All the animal experiments were approved by the Institutional Animal Ethics Committee of Tongji Hospital of Huazhong University of Science and Technology.

Consent for publication

Not applicable.

References

1. Torre LA, Bray F, Siegel RL et al (2015) Global cancer statistics, 2012. CA: a cancer journal for clinicians 65: 87-108.
2. Bray F, Ferlay J, Soerjomataram I et al (2018) Global cancer statistics 2018: GLOBOCAN estimates of incidence and mortality worldwide for 36 cancers in 185 countries. 68: 394-424.
3. Llovet J, Kelley R, Villanueva A et al (2021) Hepatocellular carcinoma. 7: 6.
4. Zhou J, Sun H, Wang Z et al (2020) Guidelines for the Diagnosis and Treatment of Hepatocellular Carcinoma (2019 Edition). 9: 682-720.
5. Zheng J, Kuk D, Gönen M et al (2017) Actual 10-Year Survivors After Resection of Hepatocellular Carcinoma. 24: 1358-66.
6. Lisker-Melman M, Jonnalagadda SJG (2005) Swimming in cloudy waters: efforts to prevent HCV-related HCC. 129: 1794-6.
7. Thiery JP, Acloque H, Huang RYJ et al (2009) Epithelial-mesenchymal transitions in development and disease. Cell 139: 871-90.
8. Valastyan S, Weinberg RA (2011) Tumor metastasis: molecular insights and evolving paradigms. Cell 147: 275-92.
9. Massagué J (2008) TGFbeta in Cancer. Cell 134: 215-30.
10. Colak S, Ten Dijke P (2017) Targeting TGF-β Signaling in Cancer. Trends Cancer 3: 56-71.

11. Derynck R, Zhang YE (2003) Smad-dependent and Smad-independent pathways in TGF-beta family signalling. Nature 425: 577-84.
12. Yuan J-h, Yang F, Wang F et al (2014) A long noncoding RNA activated by TGF-β promotes the invasion-metastasis cascade in hepatocellular carcinoma. Cancer Cell 25: 666-81.
13. Akhurst RJ, Hata A (2012) Targeting the TGFβ signalling pathway in disease. Nat Rev Drug Discov 11: 790-811.
14. Wu N, Jiang M, Liu H et al (2021) LINC00941 promotes CRC metastasis through preventing SMAD4 protein degradation and activating the TGF-β/SMAD2/3 signaling pathway. 28: 219-32.
15. Tang J, Yu B, Li Y et al (2019) TGF-β-activated lncRNA LINC00115 is a critical regulator of glioma stem-like cell tumorigenicity. 20: e48170.
16. Jiang L, Wang R, Fang L et al (2019) HCP5 is a SMAD3-responsive long non-coding RNA that promotes lung adenocarcinoma metastasis via miR-203/SNAI axis. 9: 2460-74.
17. Orom UA, Derrien T, Beringer M et al (2010) Long noncoding RNAs with enhancer-like function in human cells. Cell 143: 46-58.
18. Guttman M, Rinn JL (2012) Modular regulatory principles of large non–coding RNAs. Nature 482: 339-46.
19. Statello L, Guo C, Chen L et al (2021) Gene regulation by long non-coding RNAs and its biological functions. 22: 96-118.
20. Xiang J, Yin Q, Chen T et al (2014) Human colorectal cancer-specific CCAT1-L lncRNA regulates long-range chromatin interactions at the MYC locus. 24: 513-31.
21. Cesana M, Cacchiarelli D, Legnini I et al (2011) A long noncoding RNA controls muscle differentiation by functioning as a competing endogenous RNA. 147: 358-69.
22. Salmena L, Poliseno L, Tay Y et al (2011) A ceRNA hypothesis: the Rosetta Stone of a hidden RNA language? 146: 353-8.
23. Xu D, Dong P, Xiong Y et al (2020) MicroRNA-361-Mediated Inhibition of HSP90 Expression and EMT in Cervical Cancer Is Counteracted by Oncogenic lncRNA NEAT1. 9.
24. Huo X, Han S, Wu G et al (2017) Dysregulated long noncoding RNAs (lncRNAs) in hepatocellular carcinoma: implications for tumorigenesis, disease progression, and liver cancer stem cells. 16: 165.
25. Liang H, Yu T, Han Y et al (2018) LncRNA PTAR promotes EMT and invasion-metastasis in serous ovarian cancer by competitively binding miR-101-3p to regulate ZEB1 expression. Molecular cancer 17: 119.
26. Liang X, Wu Z, Shen S et al (2020) LINC01980 facilitates esophageal squamous cell carcinoma progression via regulation of miR-190a-5p/MYO5A pathway. 686: 108371.
27. Quagliata L, Matter MS, Piscuoglio S et al (2014) Long noncoding RNA HOTTIP/HOXA13 expression is associated with disease progression and predicts outcome in hepatocellular carcinoma patients. Hepatology 59: 911-23.
28. Wang Y, Sun L, Wang L et al (2018) Long non-coding RNA DSCR8 acts as a molecular sponge for miR-485-5p to activate Wnt/β-catenin signal pathway in hepatocellular carcinoma. Cell Death Dis 9: 851.

29. Mo Y, He L, Lai Z et al (2018) LINC01287/miR-298/STAT3 feedback loop regulates growth and the epithelial-to-mesenchymal transition phenotype in hepatocellular carcinoma cells. J Exp Clin Cancer Res 37: 149.
30. Cao L, Cheng H, Jiang Q et al (2020) APEX1 is a novel diagnostic and prognostic biomarker for hepatocellular carcinoma. Aging (Albany NY) 12: 4573-91.
31. Huang T, Wang Y-J, Huang M-T et al (2021) LINC00470 accelerates the proliferation and metastasis of melanoma through promoting APEX1 expression. Cell Death Dis 12: 410.
32. Jiang Y, Yim S-H, Xu H-D et al (2011) A potential oncogenic role of the commonly observed E2F5 overexpression in hepatocellular carcinoma. World J Gastroenterol 17: 470-7.
33. Karmakar D, Maity J, Mondal P et al (2020) E2F5 promotes prostate cancer cell migration and invasion through regulation of TFPI2, MMP-2 and MMP-9. Carcinogenesis 41: 1767-80.
34. Ren Y, Wang Y, Hao S et al (2020) NFE2L3 promotes malignant behavior and EMT of human hepatocellular carcinoma (HepG2) cells via Wnt/β-catenin pathway. J Cancer 11: 6939-49.
35. Wang C, Saji M, Justiniano SE et al (2017) RCAN1-4 is a thyroid cancer growth and metastasis suppressor. JCI Insight 2: e90651.
36. Bartel DP (2009) MicroRNAs: target recognition and regulatory functions. Cell 136: 215-33.
37. Massagué J (2012) TGFβ signalling in context. Nat Rev Mol Cell Biol 13: 616-30.
38. Bhan A, Soleimani M, Mandal SS (2017) Long Noncoding RNA and Cancer: A New Paradigm. Cancer Res 77: 3965-81.
39. Huang Z, Zhou J-K, Peng Y et al (2020) The role of long noncoding RNAs in hepatocellular carcinoma. Molecular cancer 19: 77.
40. Yang Z, Jiang S, Shang J et al (2019) LncRNA: Shedding light on mechanisms and opportunities in fibrosis and aging. Ageing Res Rev 52: 17-31.
41. Zheng Z-Q, Li Z-X, Zhou G-Q et al (2019) Long Noncoding RNA FAM225A Promotes Nasopharyngeal Carcinoma Tumorigenesis and Metastasis by Acting as ceRNA to Sponge miR-590-3p/miR-1275 and Upregulate ITGB3. Cancer Res 79: 4612-26.
42. Wu P, Cai J, Chen Q et al (2019) Lnc-TALC promotes O-methylguanine-DNA methyltransferase expression via regulating the c-Met pathway by competitively binding with miR-20b-3p. Nat Commun 10: 2045.
43. Chen X, Chen Z, Yu S et al (2018) Long Noncoding RNA LINC01234 Functions as a Competing Endogenous RNA to Regulate CBFB Expression by Sponging miR-204-5p in Gastric Cancer. Clin Cancer Res 24: 2002-14.
44. Xie Y, Hang X, Xu W et al (2021) CircFAM13B promotes the proliferation of hepatocellular carcinoma by sponging miR-212, upregulating E2F5 expression and activating the P53 pathway. Cancer Cell Int 21: 410.
45. Wang Y, Wang X, Han L et al (2020) LncRNA MALAT1 Regulates the Progression and Cisplatin Resistance of Ovarian Cancer Cells via Modulating miR-1271-5p/E2F5 Axis. Cancer Manag Res 12.

46. Sakai S, Ohhata T, Kitagawa K et al (2019) Long Noncoding RNA Acts as a Smad3 Cofactor to Facilitate TGFβ/Smad Signaling and Promote Epithelial-Mesenchymal Transition. Cancer Res 79: 2821-38.
47. Jiang L, Wang R, Fang L et al (2019) HCP5 is a SMAD3-responsive long non-coding RNA that promotes lung adenocarcinoma metastasis via miR-203/SNAI axis. Theranostics 9: 2460-74.
48. Arase M, Horiguchi K, Ehata S et al (2014) Transforming growth factor-β-induced lncRNA-Smad7 inhibits apoptosis of mouse breast cancer JygMC(A) cells. Cancer Sci 105: 974-82.

Figures

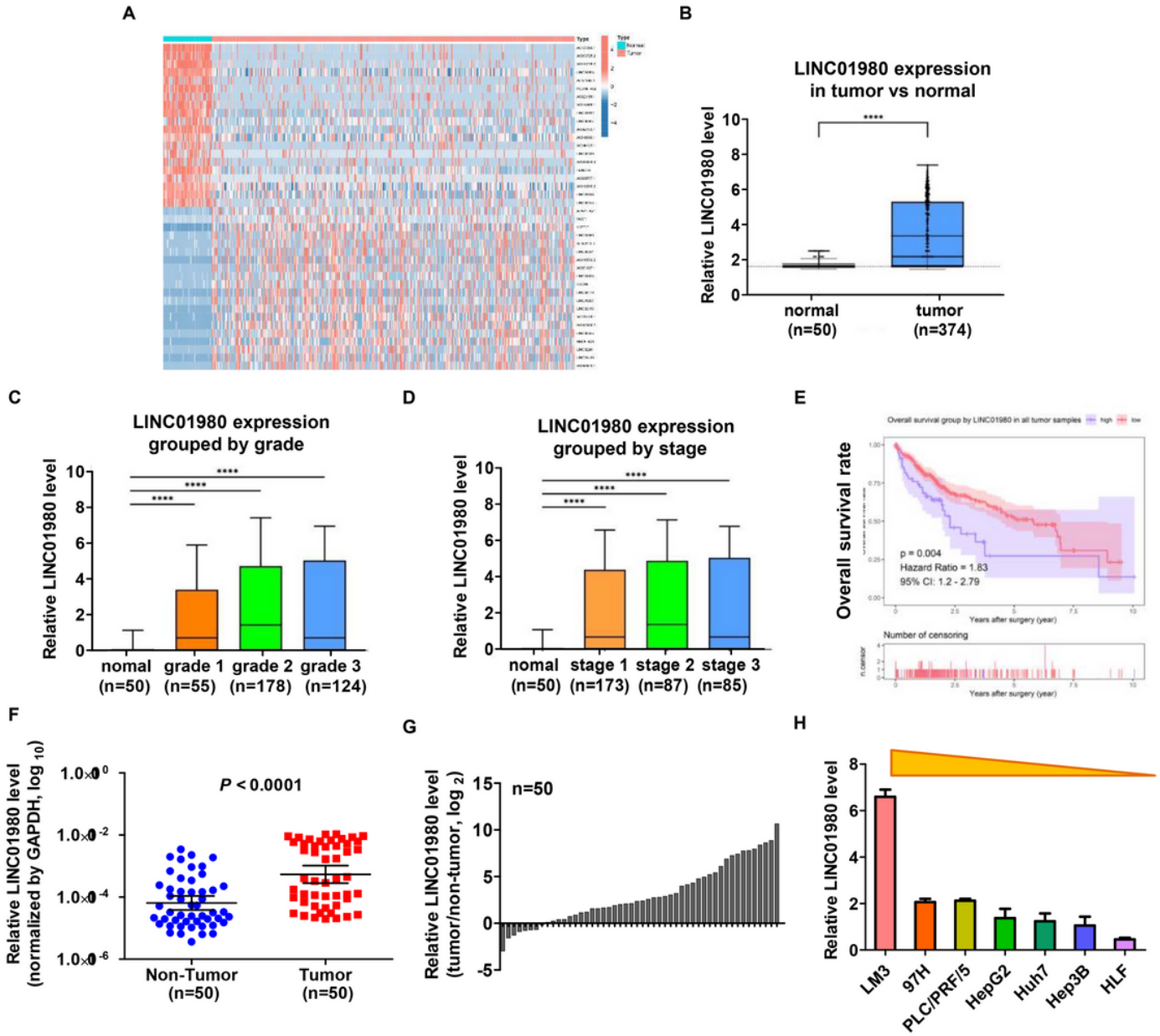

Figure 1

LINC01980 was highly expressed and related to poor prognosis in HCC. **A** Heatmap showed the up-regulated and down-regulated top 20 lncRNAs from TCGA database. **B** Bioinformatic analysis of the LINC01980 differential expression in TCGA database. **C-D** The correlation between LINC01980 and tumor grade or stage. E. The impact of LINC01980 expression on the prognosis of HCC patients. **F** The qRT-PCR analysis of LINC01980 differential expression in HCC tissues and matched adjacent non-tumor tissues (n=50). **G** The relative expression of LINC01980 in 50 paired tissues [log2(T/N)]. **H** The qRT-PCR analysis of LINC01980 in HCC cell lines with different metastasis potential. *$p < 0.05$, **$p < 0.01$.

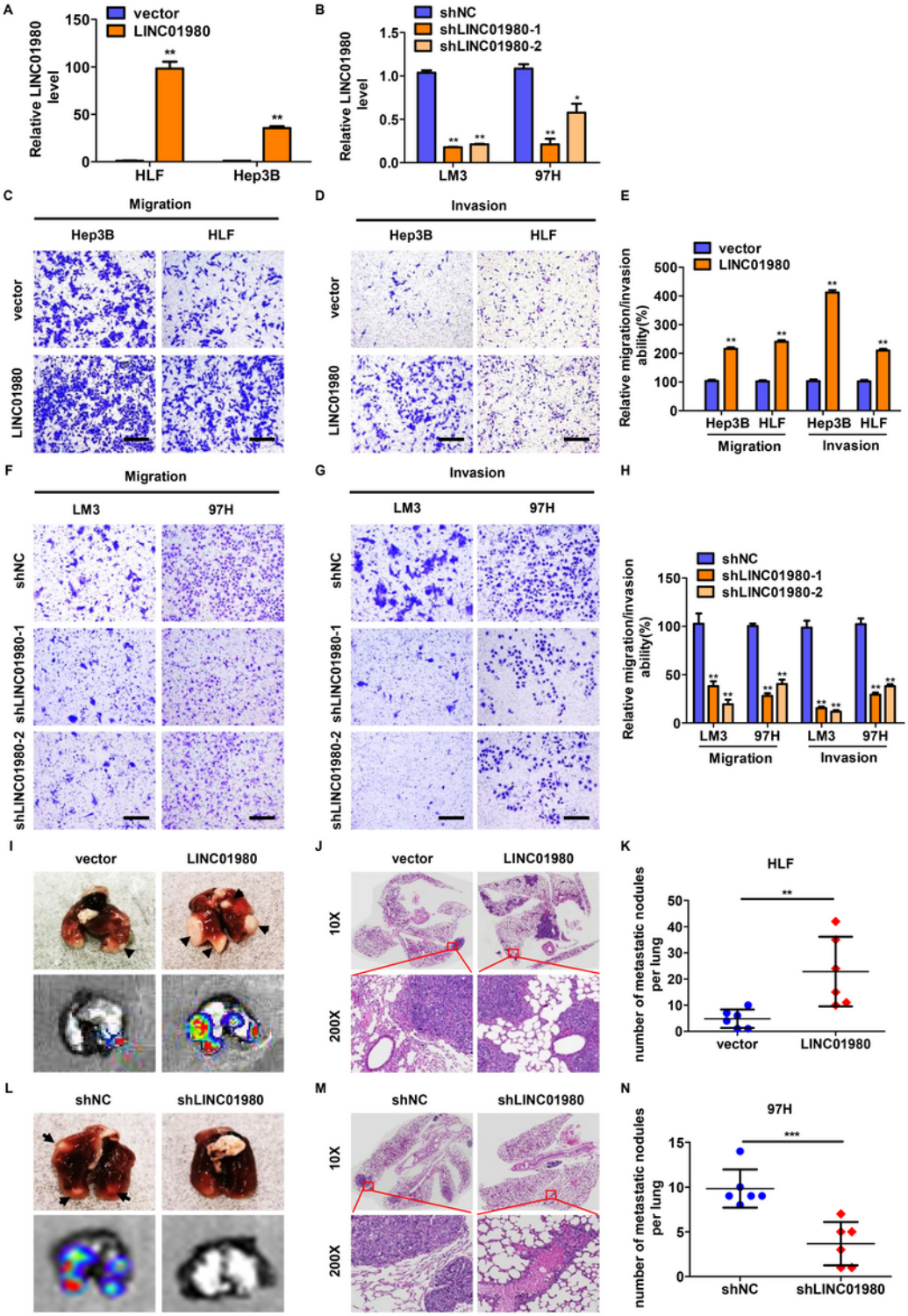

Figure 2

LINC01980 promotes HCC cell metastasis in vitro and vivo. **A-B** The qRT-PCR analysis of LINC01980 expression in HCC cells transfected with LINC01980 overexpressing (**A**) or knockdown (**B**) lentivirus. **C-H** Transwell experiments were performed to investigate the migration and invasion ability of LINC01980 overexpressing (**C-E**) and knockdown (**F-H**) HCC cells. **I-N** Lung metastasis models were performed by injected HCC cells with LINC01980 stably overexpressing or silencing into the tail veins of 6-week-old male

BALB/C nude mice. **I** and **L** Representative images of mice lungs and matched bioluminescent imaging of the different groups are presented. **J-K** and **M-N** The H&E staining showed the number of visible tumor nodules in mice lungs of the different groups. Scale bar, 100 μm. *$p < 0.05$, **$p < 0.01$.

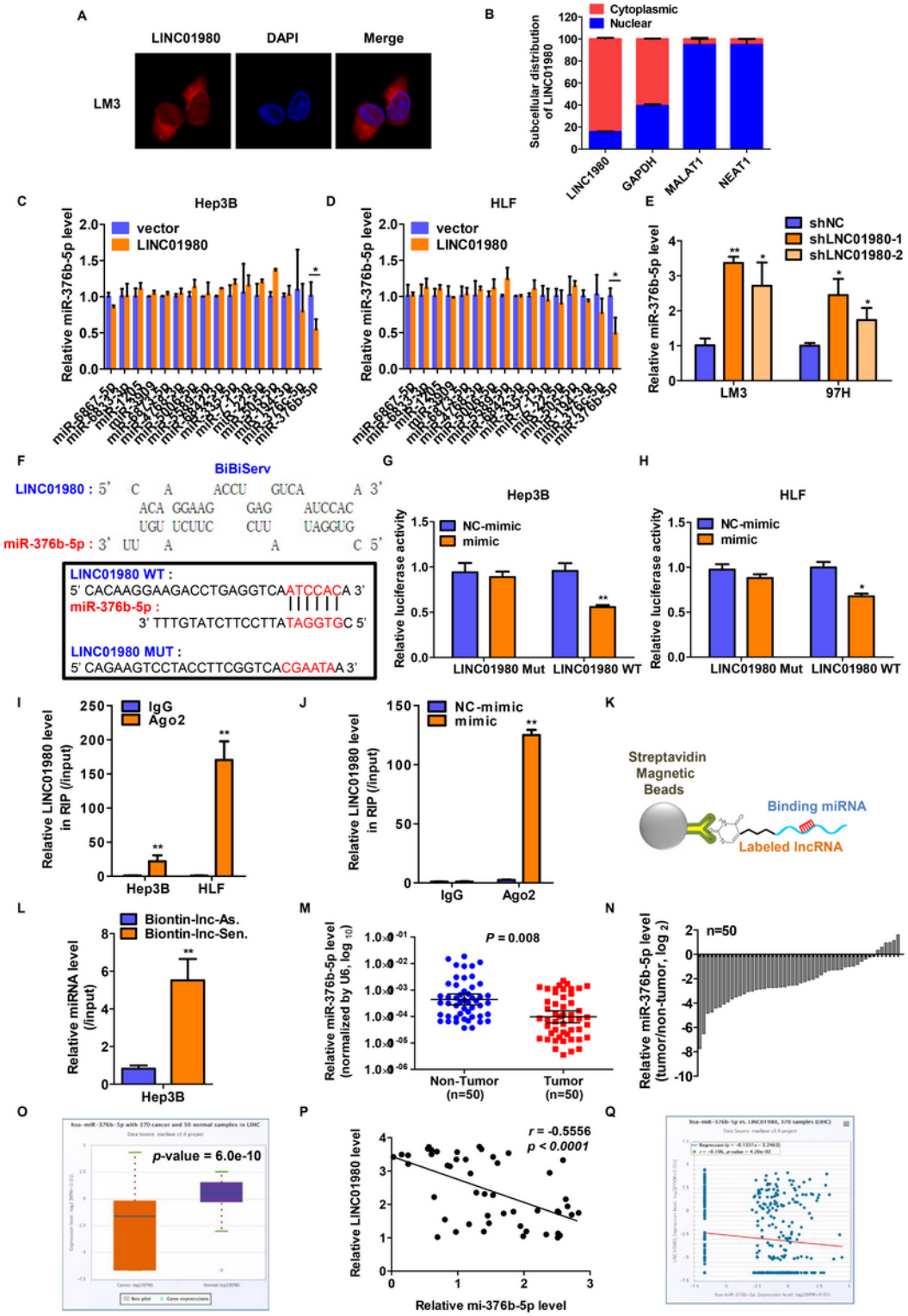

Figure 3

LINC01980 acts as a ceRNA and competitively binds miR-376b-5p. **A-B** subcellular localization of LINC01980 in LM3 cells, tested by nuclear-cytoplasmic RNA fractionation and FISH assays. **C-D** qRT-PCR

assays were conducted to screen target miRNA of LINC01980 by overexpressing LINC01980 in HCC cells. **E** The expression of miR-376b-5p in LINC01980 silenced cells. **F** The binding site between LINC01980 and miR-376b-5p was predicted by RNAhybrid and the mutated sequence of LINC01980 luciferase reporter gene was showed. **G-H** The relative luciferase activity was detected in Hep3B and HLF cells after co-transfection LINC01980 WT or MUT with miR-376b-5p mimic or NC. **I-J** Anti-Ago2 RIP assay was conducted in HCC cells transfected with mimics or not, followed by qRT-PCR to detect LINC01980. **K-L** RNA pulldown assay was conducted in Hep3B cells to prove that miR-376b-5p was specifically pulled down by biotin-labelled LINC01980 compared with LINC01980-antisense. **M** The qRT-PCR analysis of miR-376b-5p differential expression in HCC tissues and matched adjacent non-tumor tissues (n=50). **N** The relative expression of miR-376b-5p in 50 paired tissues [log2(T/N)]. **O** The expression of miR-376b-5p in HCC tissues from StarBase website. **P-Q** The correlation between LINC01980 and miR-376b-5p in tumor tissues (**P**) or StarBase website (**Q**). *$p < 0.05$, **$p < 0.01$.

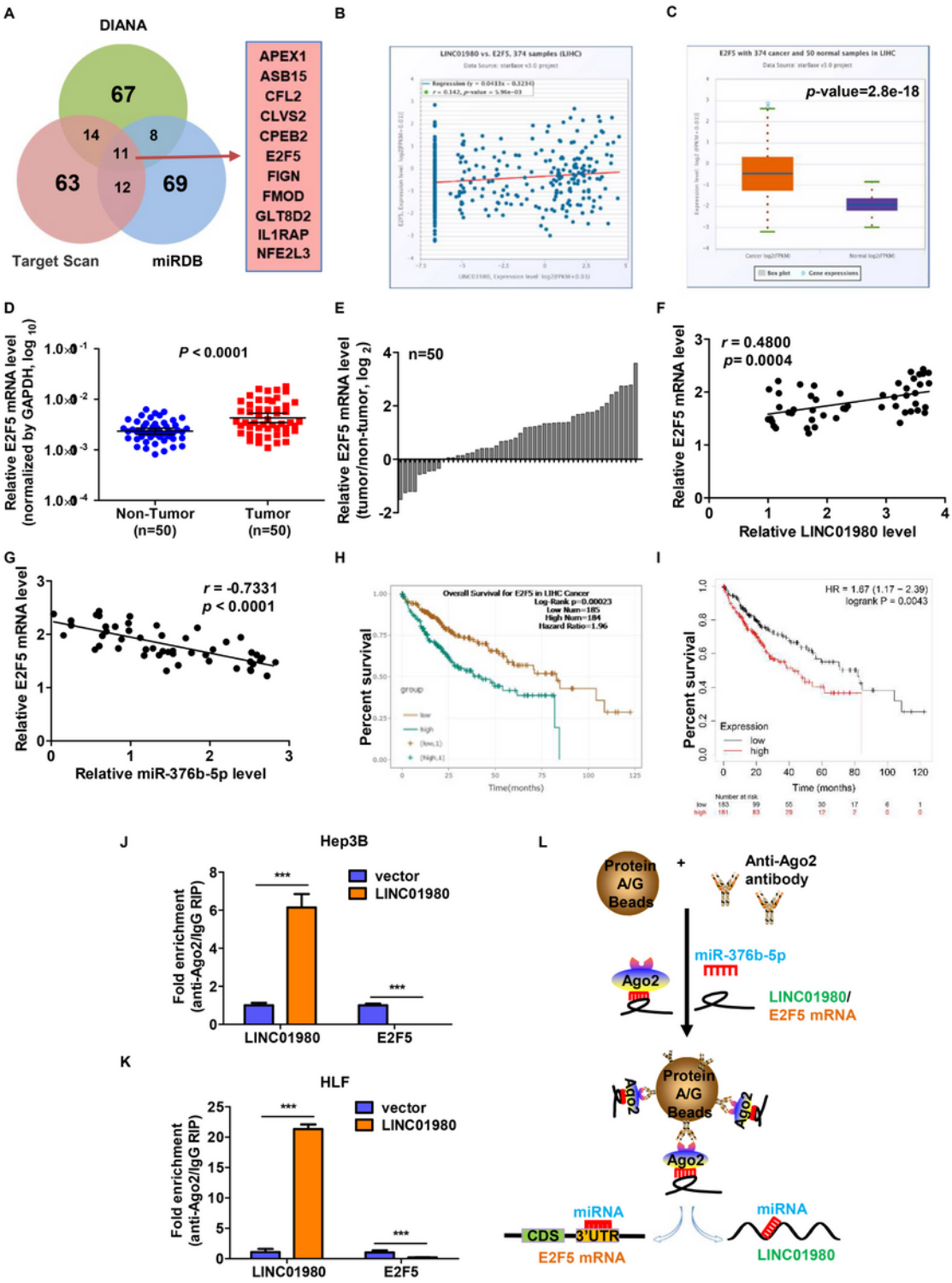

Figure 4

E2F5 is a downstream target of miR-376b-5p. **A** The potential targets of miR-376b-5p were predicted by bioinformatics databases (miRDB, DIANA, and Target Scan). **B** The correlation between LINC01980 and E2F5 was analyzed by the StarBase website. **C** The expression of E2F5 in HCC tissues from the StarBase website. **D** The qRT-PCR analysis of E2F5 expression in HCC tissues and matched adjacent non-tumor tissues (n=50). **E** The relative expression of E2F5 in 50 paired tissues [log2(T/N)]. **F-G** The correlation

between LINC01980 and E2F5 (**F**) or E2F5 and miR-376b-5p (**G**) in HCC tissues. **H-I** The prognosis analysis was conducted by StarBase (**H**) and Kaplan Meier-plotter websites (**I**). **J-K** Anti-Ago2 RIP assay was conducted in HCC cells transfected with LINC01980 overexpressing plasmid or vector, followed by qRT-PCR to detect LINC01980 and E2F5 level. **L** The RIP schematic shows that LINC01980 and E2F5 mRNA transcript competitively bind miR-376b-5p on Ago2. *$p < 0.05$, **$p < 0.01$.

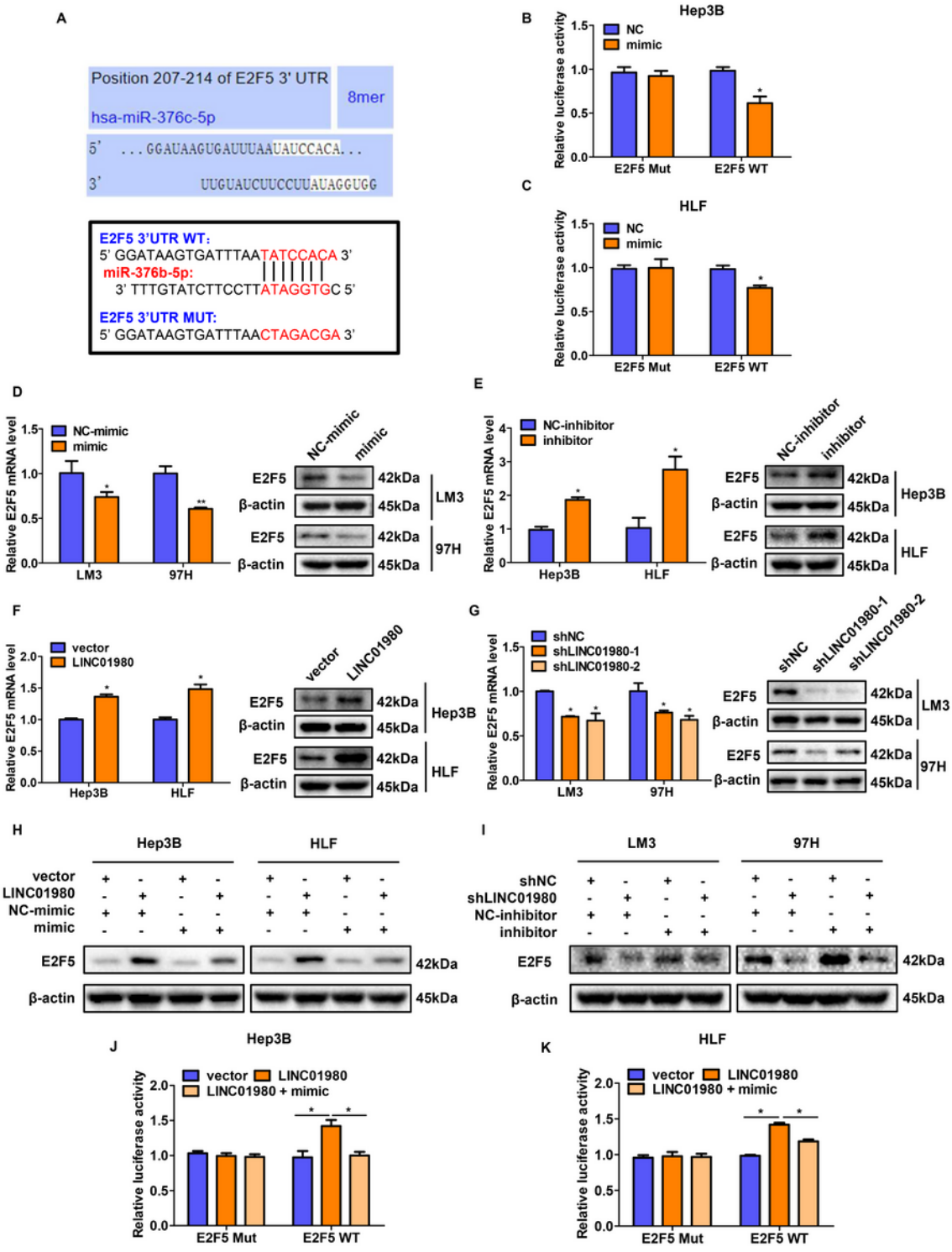

Figure 5

LINC01980 decoyed miR-376b-5p to upregulate its target E2F5. **A** the potential binding site between miR-376b-5p and 3'UTR of E2F5 we predicted by TargetScan databases. **B-C** The relative luciferase activity was detected in Hep3B and HLF cells transfected E2F5 WT or MUT together with miR-376b-5p mimic or NC. **D-E** The mRNA or protein levels of E2F5 in HCC cells transfected with miR-376b-5p mimic or inhibitor. **F-G** The mRNA or protein levels of E2F5 in HCC cells with LINC01980 overexpression or knockdown. **H-I** The protein levels of E2F5 in LINC01980 overexpressing or knockdown HCC cells together with miR-376b-5p up-regulation or down-regulation, respectively. **J-K** Luciferase activity was detected in Hep3B and HLF cells overexpressing LINC01980 after transfected E2F5 WT or MUT together with miR-376b-5p mimic. *$p <$ 0.05, **$p < 0.01$.

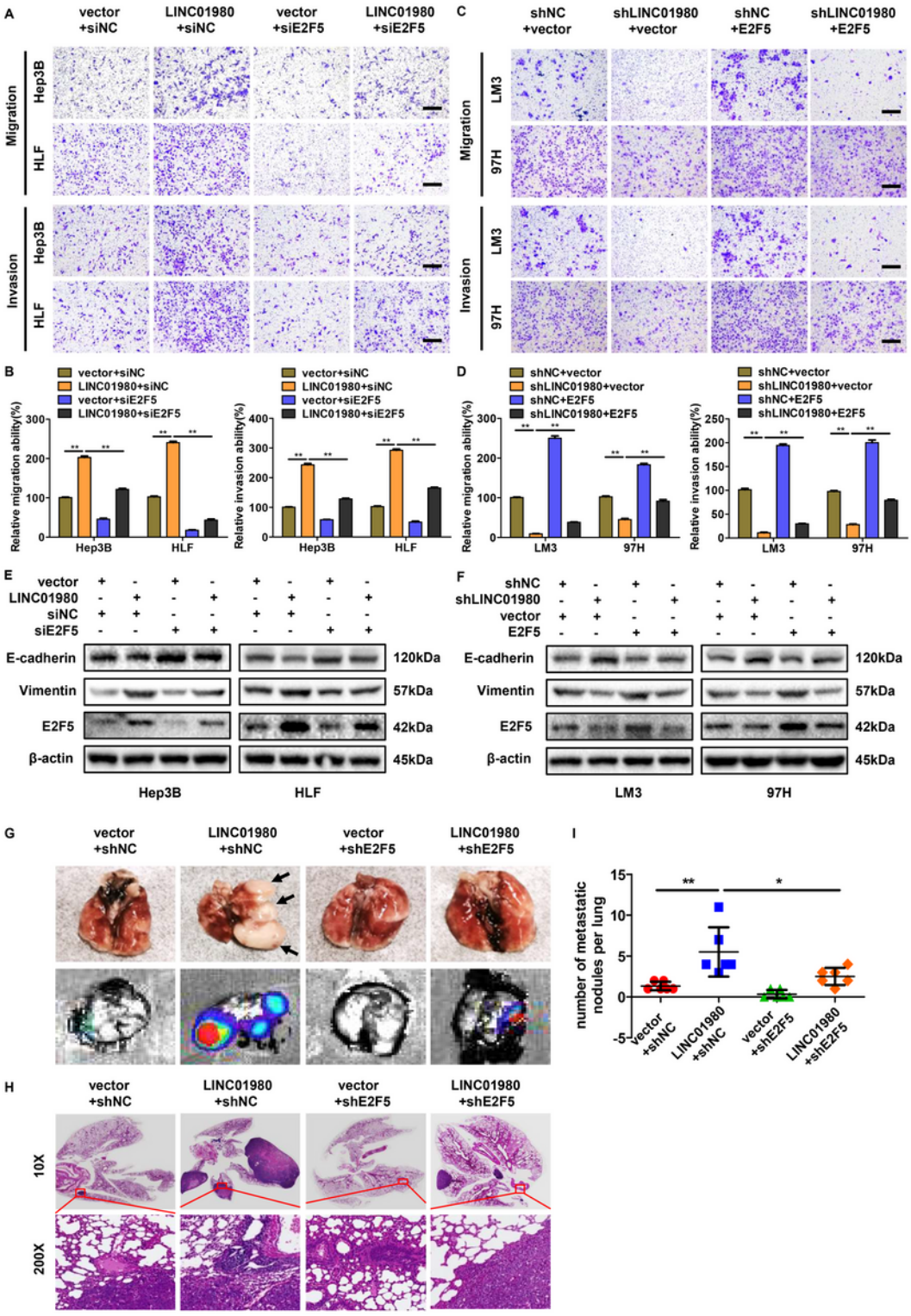

Figure 6

E2F5 is indispensable for LINC01980-mediated cell migration and invasion in vitro and vivo. **A-D** Transwell experiments were performed to assess cell migratory and invasive capabilities in LINC01980 overexpressing or silencing HCC cells, respectively. **E-F** Western blot assays were performed to assess the protein level of E2F5 and EMT markers in LINC01980 overexpressing or silencing HCC cells together with E2F5 silencing or overexpressing, respectively. **G-I** Lung metastasis models were performed. **G**

Representative images of mice lungs and matched bioluminescent imaging of the different groups are presented. **H-I** The H&E staining showed the number of visible tumor nodules in mice lungs of the different groups. Scale bar, 100 μm. Data were presented as mean ± SD of three independent experiments. *p < 0.05, **p < 0.01.

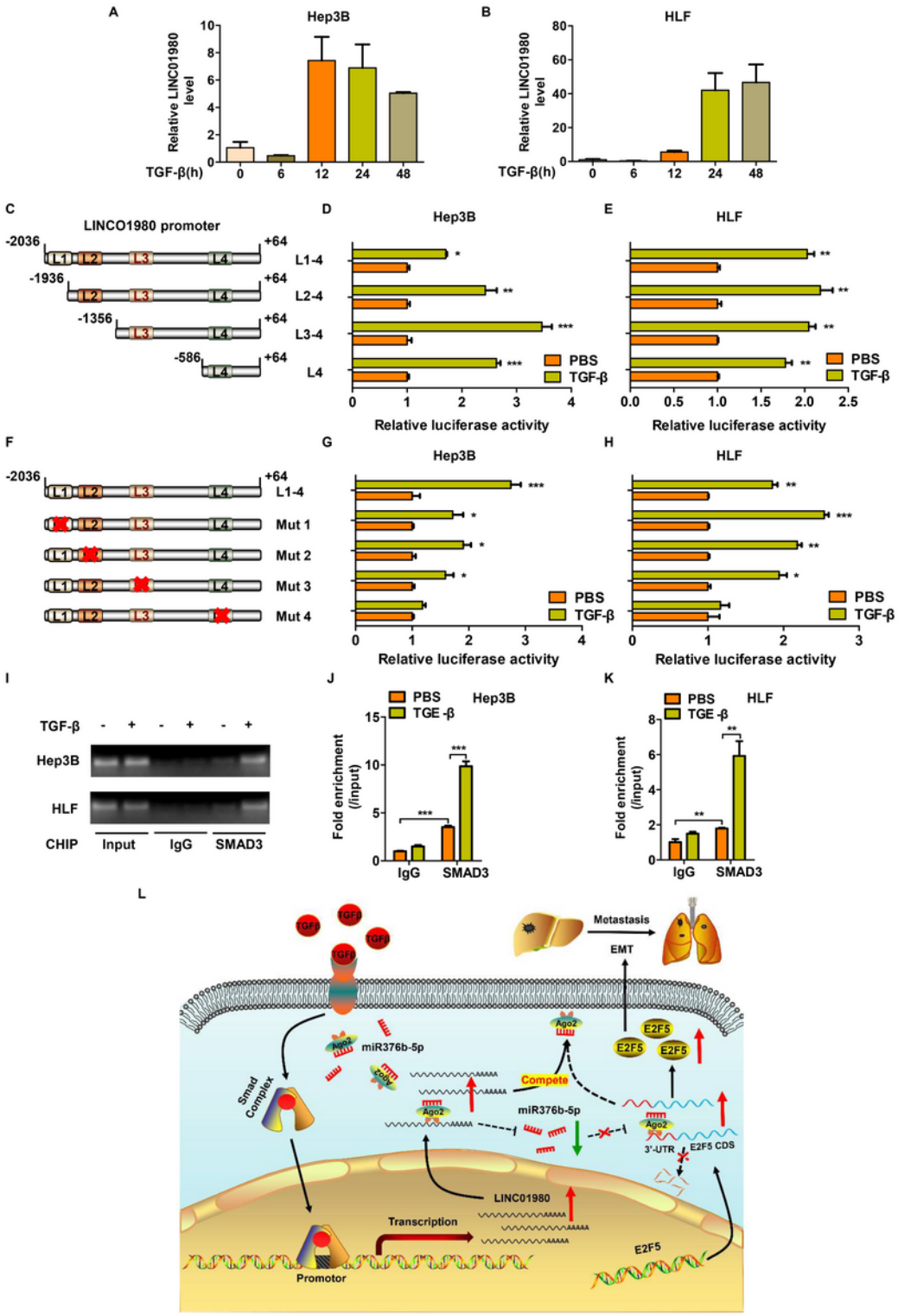

Figure 7

LINC01980 is induced by the canonical TGF-β signaling pathway. **A-B** Hep3B and HLF cells were treated with or without 10 ng/mL TGF-β for different times. Then, the levels of LINC01980 were determined via qRT-PCR. **C-H** Activities of LINC01980 promoter truncations (**C-E**) and mutations (**F-H**) in TGF-β-treated HCC cells were detected by dual-luciferase assays. **I-K** Anti-SMAD3 CHIP assays followed by semi-quantitative PCR analyses to prove that SMAD3 binds to LINC01980 promoter. **L** LINC01980 induced by TGF-beta promotes hepatocellular carcinoma metastasis via miR-376b-5p/E2F5 axis. *$p < 0.05$, **$p < 0.01$.

Supplementary Files

This is a list of supplementary files associated with this preprint. Click to download.

- SupplementaryMaterials.pdf
- SupplementaryTable2.xlsx